Chapter 3
Type II Superconductors

Abstract Superconductivity with high T_c was found in a number of alloys and compounds which displayed a strange type of behavior. They were found to be perfect diamagnetic only up to a small field, called lower critical field, B_{c1} but remained superconducting up to a high magnetic field called the upper critical magnetic field, B_{c2}. Abrikosov explained this behavior in terms of the formation of negative surface energy at the normal-superconducting interface in these materials. Beyond B_{c1} field starts entering the material in the form of flux lines each carrying a quantum of flux, $\Phi_0 = h/2e = 2 \times 10^{-15}$ T m^2. Since formation of normal zone (flux lines) reduces the energy, this, so called the "mixed state", is more stable. The flux lines form a triangular lattice and are produced by the circulating persistent currents around the normal cores. Mixed state has a fine structure with a periodicity of $<10^{-6}$ and is an intrinsic property of these so called type II superconductors. At B_{c2} the material is overtaken completely by the flux and turns normal. If a current flows in a superconductor in the mixed state the flux lines experience Lorentz force, forcing them to move. A voltage appears and the material turns normal. Flux lines are, however, pinned by impurities or imperfections introduced in the material and the critical current density is increased to desired level. Only type II superconductors are capable of carrying large currents without dissipation in presence of high magnetic field and are of technological importance.

3.1 Strange Behavior of Superconductors: Abrikosov's Concept of Negative Surface Energy

After having studied superconductivity in metals across the periodic table, and the consequent disappointment with low T_c values, the researchers in the field of superconductivity changed track and started looking for superconductivity in alloys and compounds. Superconductivity was indeed discovered in a large number of alloys and compounds. These new superconductors, however, displayed a strange behaviour in so far as they did not show perfect diamagnetism like pure metals.

R.G. Sharma, *Superconductivity*, Springer Series in Materials Science 214,
DOI 10.1007/978-3-319-13713-1_3

Instead, they exhibited partial flux penetration. At first instance it was thought to be either an experimental artifact or an impurity effect. Abrikosov [1], however, predicted in 1957 a new class of superconductors, now called type II with anomalous properties. He emphasized that it is a new class of superconductors and not a trivial impurity effect. He argued that in metal superconductors, referred to as type I superconductors, occurrence of perfect diamagnetism implies that there is positive surface energy at the normal-superconducting boundary. Let us consider a normal region in a type I superconductor in a magnetic field $B_a < B_c$ the free energy of normal regions/unit volume is greater than for the superconducting region (diamagnetic state) by $\frac{\mu_0}{2}\left(B_c^2 - B_a^2\right)$. Thus in a type I superconductor the free energy will increase if the normal regions were to grow. This is energetically unfavourable and therefore it remains superconducting until a field B_c is reached. Let us now assume a negative surface energy [2] at the superconducting—normal boundary. This will imply that the energy will reduce if normal regions are formed in the superconductor. When a field is applied, a large number of normal regions are formed resulting in a large negative energy. It thus becomes energetically favourable to allow partial flux penetration than carrying the burden of expelling the field completely.

To understand the concept of negative surface energy, we should recall that type II superconductivity is observed mostly in alloys and compounds (with a few exceptions like Nb, V and T_c) where the mean free path is very small and so is the coherence length. Thus type II superconductors are characterized by a coherence length ξ much smaller than the penetration depth λ. Let us now refer to positive surface energy in type I superconductors discussed in Chap. 2 (Fig. 2.23). Compare it with Fig. 3.1 for type II superconductors where $\xi \ll \lambda$ resulting in a negative surface energy close to the N–S boundary. Here we see that well inside the material the two contributions to free energy namely, electron ordering contribution and the magnetic contribution cancel each other but close to the boundary there is now a net negative energy.

3.2 Lower and Upper Critical Magnetic Field

Figure 3.2 shows the magnetic phase diagrams of the type I and type II superconductors. Figure 3.2a is the same as Fig. 2.5 for the type I superconductor whereas Fig. 3.2b is the phase diagram for type II superconductors. As seen in the figure, type II superconductors are now characterized by two critical magnetic fields instead of one for type I. The type II superconductor shows perfect diamagnetism only up to a magnetic field, B_{c1}, called the lower critical magnetic field. This field is a fraction of the thermodynamical magnetic field B_c. Material however stays superconducting (zero resistance) up to a magnetic field which is significantly higher than B_c and is called upper critical magnetic field, B_{c2}. A type II superconductor can thus sustain a very high magnetic field and can still carry large current. It is for this reason that only type II superconductors are of technological

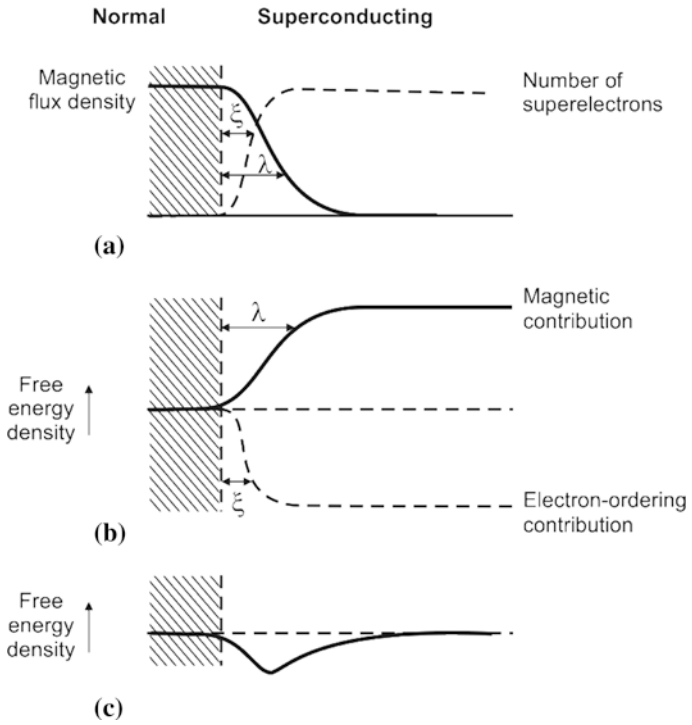

Fig. 3.1 Lowering of energy, due to pair formation, is more than the increase in energy due to magnetic contribution close to the N–S boundry resulting in a negative surface energy [2, p. 175]. **a** Penetration depth and coherence range at boundary. **b** Contributions to free energy. **c** Total free energy (With permission from Elsevier)

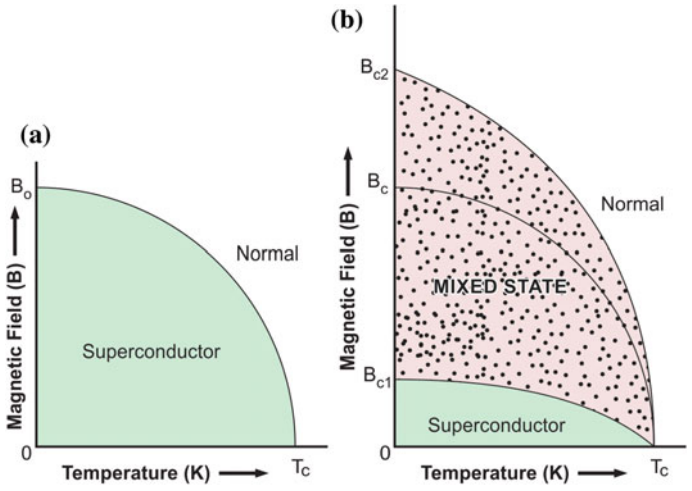

Fig. 3.2 Magnetic phase diagrams of type I (**a**) and type II (**b**) superconductors

importance and are widely used for magnet construction. All the three critical magnetic fields are inter-related in the following way;

$$B_c = [8\pi(g_n - g_s)]^{\frac{1}{2}} \tag{3.1}$$

$$B_{c1} = \frac{B_c}{\left(\kappa\sqrt{2}\right)^{0.65}} \tag{3.2}$$

$$B_{c2} = \left(\sqrt{2}\right)\kappa B_c \tag{3.3}$$

$(g_n - g_s)$ is the energy difference between the normal state and the superconducting state and κ is the G–L parameter ($=\lambda/\xi$). As κ increases B_{c1} decreases with respect to B_c and B_{c2} increases. The value of κ is given by the G–L theory:

$$\kappa = \frac{\left(\sqrt{2}\right)2\pi\lambda^2\mu_0 B_c}{\Phi_0} \tag{3.4}$$

where $\Phi_0 = h/2e = 2 \times 10^{-15}$ T m^2, the flux quanta. It is pertinent to note here that in alloys electron mean free path is short which means the coherence length ξ decreases and λ increases thus making κ large. For type I superconductor $\kappa < 0.71$ and for type II $\kappa > 0.71$. However, κ can be more than 0.71 even for pure metals in exceptional cases as shown in Table 3.1.

For pure metals κ increases with impurity and thus with normal state resistivity as per the relation below:

$$\kappa = \kappa_0 + 7.5x\sqrt{10}x10^5\gamma^{\frac{1}{2}}\rho \tag{3.5}$$

where κ_0 is the value of κ for pure metal, ρ and γ are normal state resistivity and coefficient of electronic specific heat respectively. Further, some metals and alloys behave like type I superconductor at T_c but turn type II at lower temperature. For example $Pb_{0.99}$ $Tl_{0.01}$ $\kappa = 0.58$ at T_c (=7.2 K) but increases to 0.71 at $T = 4.3$ K. For pure vanadium $\kappa = 0.85$ at T_c (=5.4 K) and increases to 1.5 at $T = 0$ K.

Table 3.1 κ values for type II pure metal superconductors

Metal superconductor	κ value
Nb	0.78
V	0.85
Tc	0.92

3.3 The Mixed State

It will be interesting to know what happens to a type II superconductor between the lower critical field B_{c1} and the upper critical field B_{c2}. The existence of a negative surface energy at the N–S boundary favours partial field penetration of the material. As shown in Fig. 3.3, between B_{c1} and B_{c2} the material undergoes 'mixed state'. It is energetically favourable that the flux lines, each carrying a unit quantum of flux Φ_0 (=$h/2e$) parallel to the applied field penetrate the material. These flux lines form a triangular lattice and are normal cores of small dimension of the order of diameter 2ξ. Mixed state is a fine structure with a periodicity of $<10^{-6}$ and a is an intrinsic property of type II superconductors.

The favourable configuration for the normal cores to thread the superconductor is a cylinder with a maximum surface to volume ratio, parallel to the applied field. Each flux line is produced by a vortex of persistent current with a sense of rotation opposite to the surface screening current. The material still remains diamagnetic being protected by the surface screening current, and the supercurrent still flows. In type II superconductors current flows through the entire cross section as compared to type I where the current flows along the surface. As field strength increases the density of normal cores increases at the expense of superconducting volume fraction and at the upper critical field B_{c2} the entire structure collapses. The material turns normal.

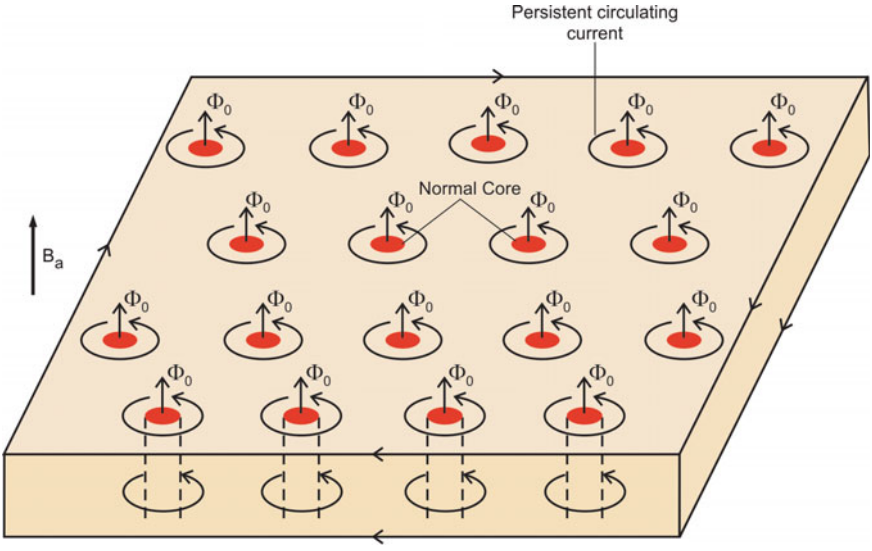

Fig. 3.3 Between B_{c1} and B_{c2} a type II superconductor undergoes mixed state. The material is threaded by *flux lines* (Φ_0) produced by vortices of persistent current with a sense of rotation opposite to surface screening

3.4 Current Flow and Mixed State

Type II superconductors are known to carry very large current in presence of high magnetic fields. Let us see how current is carried by the superconductor in mixed state. In the mixed state the current is not impeded by the presence of flux lines, the size of the normal cores being very small ($\sim 2\xi$). The vortices repel each other so that the normal cores are confined to small area and the current flows without hindrance as long as it does not disrupts vortices. The flux lines, however, experience a Lorentz force, F_L under the influence of the transport current and the perpendicular transverse field which tries to move it in the third perpendicular direction (Fig. 3.4). The movement of the flux lines generates a finite voltage and a resistance appears. The flux lines are however held back by the crystal lattice through a pinning force F_P. Imperfections, defects and impurities are introduced into the superconducting materials to create pinning sites. The pinning force is thus increased significantly and the superconductor can carry a much larger current.

The flux lines do not move until the time Lorentz force becomes equal to the pinning force. This happens at a current density value, called the critical current density J_c. Once the J_c is exceeded flux lines start moving, a voltage appears and the material reverts back to normal state.

Figure 3.5 shows two typical plots of J_c versus the magnetic field. The lower plot is for a clean, defect free type II superconductor and the upper plot is drawn for the dirty' superconductor with defects or the so called pinning centres. As seen from the figure J_c drops sharply to low value for a pure superconductor at low field and is hardly of use for practical applications. The dirty superconductors, normally referred to as "hard superconductors" with pinning sites (defects) on the other hand carries large useful current at high magnetic field. Defects are, in fact, substituted intelligently in a

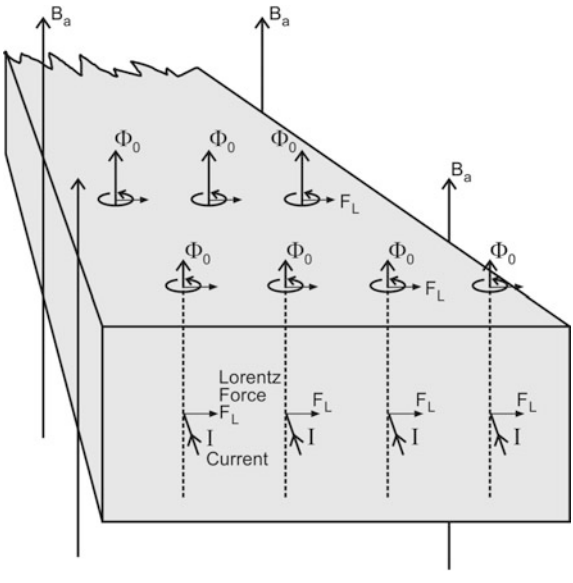

Fig. 3.4 In the mixed state *flux lines* (*normal cores*) experience Lorentz force (F_L) when a longitudinal current flows through the superconductor. Movement of *flux line* is prevented by flux pinning mechanism

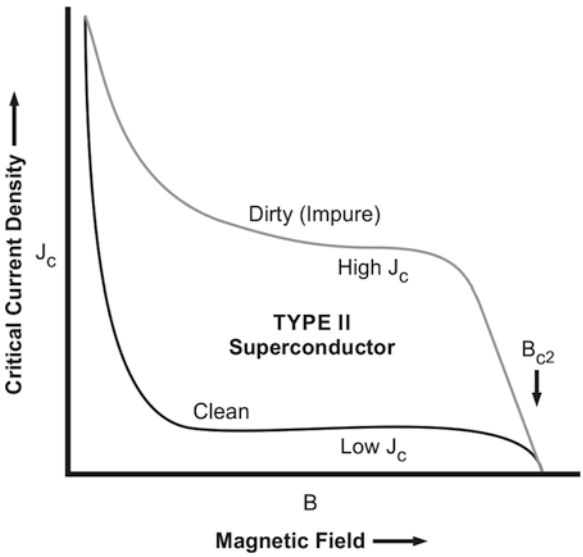

Fig. 3.5 J_c versus magnetic field for type II superconductors in clean limit and the dirty limit with pinning centres. J_c in both the cases drops to zero at B_{c2}. Notice high J_c in dirty (hard) superconductors

superconductor to create pinning sites which increase the pinning force many fold. The critical current increases dramatically whereby the superconductor can be used for magnet applications like in accelerators and the fusion reactors where the superconducting cables carry several kA current and in high magnetic field.

3.5 Measuring Transport Critical Current

Critical Current density is the single most important parameter for characterizing a superconducting (multifilamentary) wire against the magnetic field. Experimentally, the superconducting wire sample is mounted on a sample probe shown schematically in Fig. 3.6 in a hair-pin geometry. While measuring critical current in a MF wire with several concentric layers of filaments around the central core it is important that the voltage contacts are made far away from the current contacts. There is a current transfer length which can be many times the wire diameter depending upon the matrix resistance. All the layers of filaments must share the current uniformly. Voltage contacts are in fact made on the horizontal part of the sample which is kept in the perpendicular magnetic field. The sample is kept dipped in liquid helium at 4.2 K. A variable dc current is passed through the sample from a power supply and the voltage across the sample is monitored using a nano-voltmeter. There is practically no voltage across the sample with increasing current until a current equal to critical current I_c is reached. There is a sharp jump in voltage at I_c as shown in Fig. 3.7. This voltage rise is caused by flux flow resistivity which is different from the Ohmic resistivity and is proportional to the normal state resistivity. I_c is determined at different values of the magnetic field. It is advisable to start from the highest

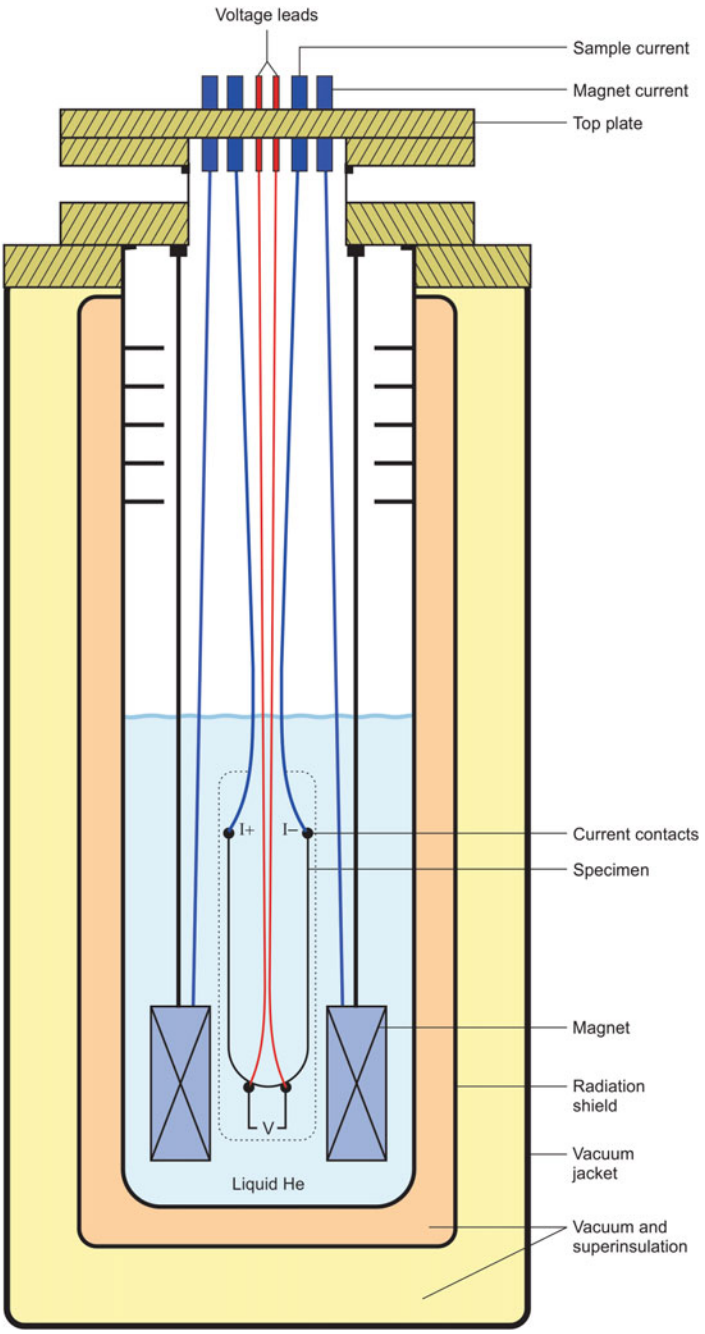

Fig. 3.6 A schematic of the superconducting magnet system used for critical current measurement. Voltage contacts on the sample are made far away from the current contacts

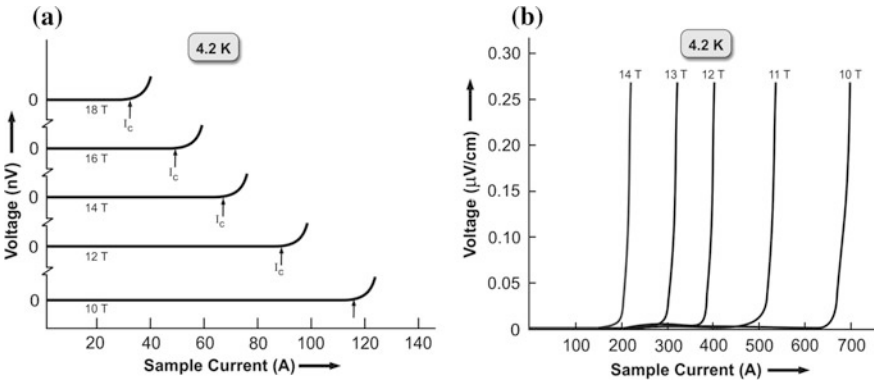

Fig. 3.7 Typical critical current, (I_c) plots at different fields. I_c decreases as the magnetic field increases

magnetic field so that the current to be passed is minimum. As the field is reduced sample carries larger currents and so also the possibility of sample burnt-out. A shunt across the sample is therefore always advisable to save the sample from burnt-out. The criterion to determine I_c is usually 0.1–0.01 μV/cm voltage drop across the sample. The critical current density, J_c is calculated by dividing I_c by the area cross section of the wire.

3.6 Magnetization in Type II Superconductors

A type II superconductor behaves exactly like type I below the critical field B_{c1} and is a perfect diamagnet with magnetization equal to $-B_a$. Beyond B_{c1} flux lines start penetrating the material (mixed state) and the magnetic flux inside the material is no longer zero as shown in Fig. 3.8a. As the magnetic field is increased magnetic flux density rises and continues till B_{c2} is reached. The material is completely taken over by the flux, turning it into the normal state. The curve retraces its reverse path in pure ideal superconductors. The corresponding magnetization versus field behaviour is shown in Fig. 3.8b. As shown, magnetization increases with magnetic field until B_{c1} and starts decreasing in field higher than B_{c1} and continues to decrease until it becomes zero at B_{c2}. Between B_{c1} and B_{c2} flux lines (normal cores) enter the material. The density of flux line is governed by the equilibrium between the reduction in free energy and the mutual repulsion between the vortices. In increasing field, normal cores pack closer together, so the average flux density increases in the material and the magnetization decreases. At B_{c2} there is a discontinuous change in the slope of the flux density and the magnetization. The material now is in normal state with flux density equal to $\mu_0 B_a$ and magnetization zero.

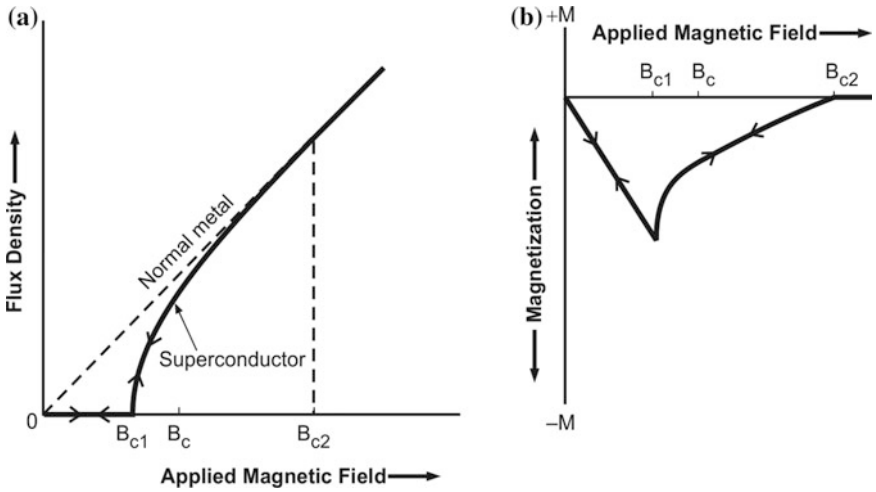

Fig. 3.8 **a** The magnetic flux density inside a type II superconductor is zero up to B_{c1} and increases in higher field. At B_{c2} flux penetrates the whole of the material. The process is reversible in ideal pure material. **b** Negative magnetization increases with magnetic field, peaks at B_{c1} and then decreases to zero at B_{c2}. This process too is reversible for pure ideal material

Magnetization measurement can be used for the determination of κ by finding the slope of the M–H curve near the field B_{c2} as per the formula

$$\left[\frac{dM}{dH}\right]_{B_{c2}} = \frac{-1}{1.16(2\kappa^2 - 1)} \tag{3.6}$$

The procedure is, however, valid only if the magnetization is reversible. The same curve should be traced while increasing and decreasing the magnetic field.

3.6.1 Irreversible Magnetization

Only ideal type II superconductors without pinning show reversibility but real type II superconductors (hard superconductors) show irreversibility in their magnetization behaviour as shown in Fig. 3.9. The reason for this magnetic irreversibility is that the flux lines or the normal cores are pinned in the bulk by imperfections and are not free to move. Consequently on increasing the field from zero there is no sudden entry of flux inside the material at B_{c1}. Thus there is rounding in the flux density and the magnetization curves at B_{c1}. Likewise on reducing the field from above B_{c2}, the two curves do not retrace their paths, but show hysteresis instead. Flux may be left trapped permanently as some flux line remain pinned down and are not able to detach and move out. Imperfections like dislocations, grain boundaries

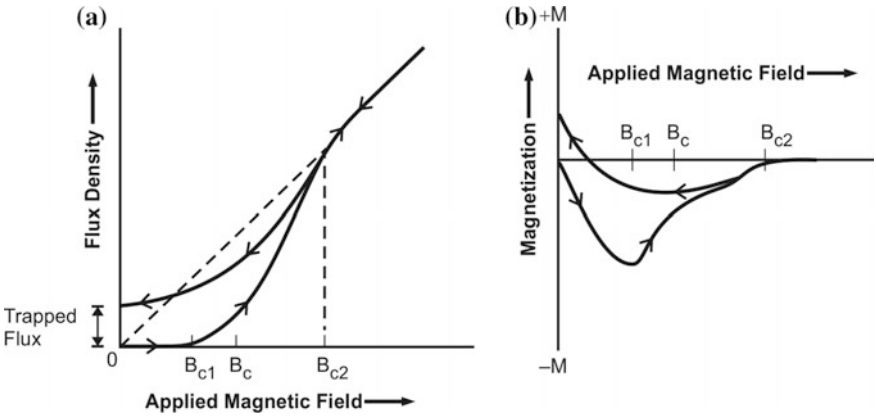

Fig. 3.9 A real type II superconductor has imperfection and show magnetic irreversibility in flux density (**a**) and in magnetization (**b**). Material can retain finite flux and magnetization even after the field is reduced to zero

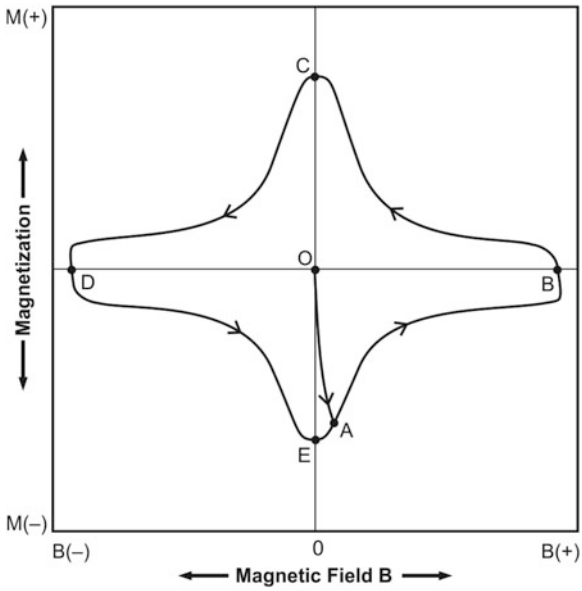

Fig. 3.10 Typical plot of magnetization versus magnetic field of a multifilamentary hard superconductor between $+B$ and $-B$. Starting from $M = 0$ to $B = 0$ point the curve traverses an irreversible path showing hysteresis. M does not drop to zero even at $B = 0$ after tracing the full cycle

and impurities can cause this type of magnetic irreversibility. The magnetic field has to be reversed to bring down magnetization M to zero but the situation at $B = 0$ and no trapped flux is retrieved only by warming the material to normal state.

Figure 3.10 shows a typical magnetization versus magnetic field loop observed in a multifilamentary conductor. To draw the full M–B loop we start from point O ($M = 0$, $B = 0$). The negative magnetization M increases with field up to the field B_{c1} (point A) and starts decreasing with the further increase of the field. Magnetization

drops to zero at B_{c2} (point B). The anomalous behaviour of these hard superconductor is that when the field starts decreasing the M–B curve does not retrace the earlier path. Instead magnetization changes sign and starts increasing to oppose the changing magnetic field attaining a peak value at C. Now if we reverse the direction of the magnetic field and start increasing it, M again drops to zero at point D. With the decreasing field M again increases in the negative direction to a peak value at point E. Thus we find that even after a full cycle from $+B$ to $-B$, the magnetization does not drop to zero at zero field. Warming of the superconductor to normal state seems to be the only way-out.

Notice that the curve is almost a straight line till a small field ($=B_{c1}$) and then it traverses an irreversible path showing hysteresis. It is seen from Fig. 3.10 that the irreversibility behavior is associated with the hysteresis and the consequent dissipation. It is interesting to note that the curve is not symmetric around the horizontal axis. This asymmetry is caused by the magnetic moments produced by the surface screening currents opposing the flux entry. Area of the hysteresis loop is the measure of the dissipation. The dissipation can be estimated from the area of the loop using the formula:

$$Q_{\text{hys}} = \oint M(B)\mathrm{d}B \tag{3.7}$$

This energy dissipation appears as frictional heat and is caused by the movement of the flux bundles in and out of the conductor. This is important for superconducting magnets in accelerators where the conductor is exposed to time-varying field. Precise calculation of heat generation is thus extremely important to work out the cryogenic refrigeration requirement. Hysteresis is an indication of an effective pinning of flux lines by imperfections which causes sharp increase of critical current density in type II superconductors, making them most suitable for magnet applications.

3.6.2 Bean's Critical-State Model and Magnetization

Superconducting magnets built during initial years during 1960s using hard superconductors performed poorly and quenched at operating currents far below the expected values. Flux jumping was found to be the main reason behind this disappointing performance, which arises because of the magnetization currents penetrating the surface deeper as the external field keeps increasing. The problem was solved in the subsequent years and ingenious techniques were perfected to produce conductors in a particular configuration which show no flux jumping and the magnets perform just as predicted. AC losses in hard superconductors is another problem faced and is a manifestation of the magnetization effects too.

The first phenomenological theory of magnetization was given by Beans [3, 4]. Even though the mixed state is well explained by the vortex structure postulated by

Abrikosov and verified experimentally, Bean assumed a 'filamentary mesh structure' (also referred to as 'Sponge model') postulated by Mendelssohn [5] for the sake of simplified calculations. According to this model the mesh consists of filaments which have diameter less than the London penetration depth. These filaments sustain supercurrent up to a critical current density J_c which is a function of magnetic field and becomes zero at the critical field of the filament. The sponge model is equivalent to a picture of multiply connected internal structure of high critical field material surrounded by a matrix of soft superconductor with low critical magnetic field.

Bean had, however, assumed that the critical current density is independent of the magnetic field which would simply mean that the field is far less than the critical field of the filaments. He also envisaged that the mesh interstices are filled with soft superconductor of critical field B_c which shields the material against the magnetic field up to B_c but the shielding beyond B_c is provided by the magnetizing currents induced in the filaments at a critical value J_c in a depth necessary to reduce the field to B_c. Bean drew the magnetization curve of a virgin hard superconductor cylinder of radius R in a magnetic field parallel to the axis by calculating internal field B_i as a function of external field B_e and the position of the superconductor.

$$4\pi M = \frac{\int_0^v (B_i - B)\mathrm{d}v}{\int_0^v \mathrm{d}v} \tag{3.8}$$

where v is the sample volume. For field less than B_c the shielding will be full if the radius R is much greater than the London penetration depth, that is

$$B_i = 0,\ 0 \le r \le R \text{ and } 0 \le B \le B_c \tag{3.9}$$

For field greater than B_c the soft superconductor surrounding the filaments becomes normal and for higher fields shielding currents are induced in the filaments flowing within a depth D_p, given by the circuital form of Ampere's law

$$D_p = 10\,(B - B_c)/4\pi J_c \tag{3.10}$$

This field dependent and macroscopic penetration depth is an interesting result of this model. Here we can define a new field $B^* = 4\pi J_c R/10$. This step simplifies the analytic expressions and B^* signifies the field that should be applied in excess of the bulk critical field which induces magnetization current to flow throughout the entire sample. Under such condition the penetration depth D_p will simply be equal to R. When all the bulk superconducting characteristics are destroyed, only shielding currents flow through the filaments under different conditions of external field.

$$B_i = B - B^*(1 - r/R); \quad 0 \le r \le R \quad B^* + B_c \le B \tag{3.11}$$

After a few mathematical steps the expressions for magnetization turn out to be

$$\text{(i)} \quad \text{For } 0 \le B \le B_c \quad 4\pi M = -B \tag{3.12}$$

$$\text{(ii)} \quad \text{For } B_c \le B \le B^* + B_c \quad 4\pi M = -B + \frac{\left(B^2 - B_c^2\right)}{B^*} + \frac{\left[B_c^2(3B - 2B_c) - B^*\right]}{3B^{*2}} \tag{3.13}$$

$$\text{(iii)} \quad \text{For } B \ge B^* + B_c \quad 4\pi M = -B^*/3 \tag{3.14}$$

The most striking result of this model is that the magnetization in hard superconductors is dependent on the macroscopic dimension of the sample. Rightly so, because critical current is carried by all the filaments which are proportional to the sample size. There is an excellent fit between the experimental magnetization data on Nb_3Sn specimens and the theoretical calculations.

The essence of Bean's critical state model thus turns out to be (i) that each hard superconductor is characterized by a limiting critical current density $J_c(B)$ and (ii) that any smallest electromotive force induces this full current that flows locally. The consequences of this model are that the regions inside a superconductor not experiencing magnetic field will carry zero current, full current at J_c will flow in regions perpendicular to the field axis. The polarities of the current depend on the polarity of the electromotive force caused by the earlier field change. The field profile in a slab of large dimensions along the Y and Z axes and finite thickness, 2a along the x-axis is shown in Fig. 3.11a for $B = 0$, $B = B^*/2$, $B = B^*$ and $B = 2B^*$. The magnetic field is parallel to the surface. The corresponding critical currents

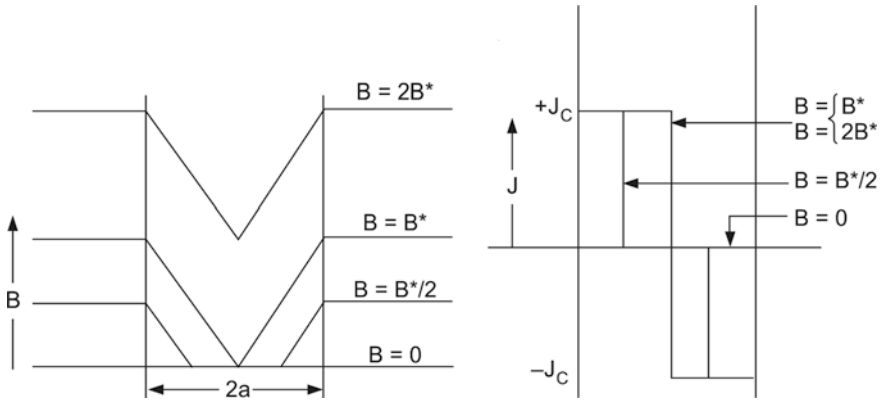

Fig. 3.11 The local field and critical current density configuration in a hard superconductor for increasing external field, $B = 0$. $B = B^*/2$, $B = B^*$ and $B = 2B^*$ in Bean's model. The J_c is assumed independent of field [4]. (With permission from APS) http://journals.aps.org/rmp/abstract/10.1103/RevModPhys.36.31

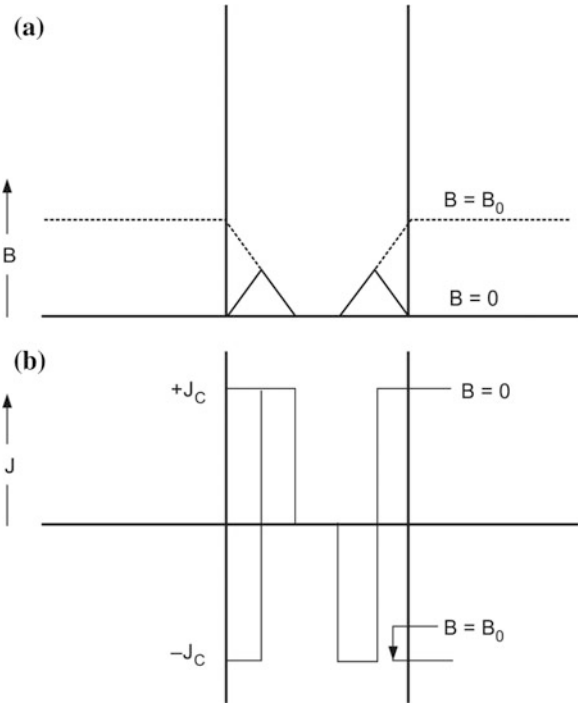

Fig. 3.12 Local fields (**a**) and current density (**b**) configuration in the slab after a field B_0 has been applied and removed [4]. (With permission from APS) http://journals.aps.org/rmp/abstract/10.1103/RevModPhys.36.31

with opposing polarities ($+J_c$ and $-J_c$) for different fields are shown in Fig. 3.11b. It can be noticed that the polarities of the critical currents along the outer and inner surface sheaths on the right and left of the mid-axis are in opposite directions.

Figure 3.12 shows the plots of the local field and critical current density in a slab of hard superconductor after a field B_0 is applied in a virgin state and removed. When the field B_0 is applied it penetrates the slab to a depth determined by the critical current to oppose this field shown in Fig. 3.12a. As we remove the field an electromotive force is generated directed in opposite direction to the one at the time of increasing field. As a result, the surface currents reverse as shown in Fig. 3.12b wherein the two surface sheaths have oppositely directed currents. The remnant flux density or the trapped flux as seen in Fig. 3.12a is exactly half the flux penetration at $B = B_0$.

3.6.3 Kim Model

Kim et al. [6] generalized Bean's critical state model and assumed that the entire region of the superconductor carries critical current which is determined only by the local field in the region. They compared experimental data on a thin walled hollow cylinder with theory. When an increasing external field (along the axis) is applied, currents are induced in the surface to counter the field. As the field keeps increasing

current penetrates the specimen deeper inside, eventually reaching a critical state. Any further increase in the field brings down the critical current density. Based upon their experimental data on hollow Nb-Zr and Nb_3Sn tubes, they postulated that the critical state is a body current in saturation and the concept of critical current applies to each macroscopic part of the sample. This critical current density is unique and a function of local magnetic field only. The state of magnetization can then be determined from this unique $J_c(B)$. A rapid sweep in the magnetic field in critical state generates an electric field which may result in a normal current flow and heating. The heating is found severe in regions where the magnetization curve is steep. This is supported by experiments which indicate that a critical state is difficult to be realized when the magnetization curve is steep. This implies that going from one critical state to another is very difficult unless the heat generated by the normal current is dissipated away fast. If the heat removal is not fast enough, the raise in temperature might quench a part of the superconductor which in turn will generate more heat. Since this additional heat is proportional to M^2, flux jumps have been found frequent in materials with large magnetization. This is the primary reason why the critical state is difficult to be realized in bulk material of large dimensions. Another interesting result of Kim model is that Lorentz force is an important parameter for the determination of the critical current density. They found a simple relationship

$$\alpha(T) = J_{cr}(B + B_0) \tag{3.15}$$

where $\alpha(T)$ and B_0 are constants. Parameter $\alpha(T)$ is strongly dependent on temperature and structure sensitive. The strong temperature dependence of $\alpha(T)$ and the fact that the critical current decays slowly in hard superconductors prompted Anderson [7, 8] to propose the theory of 'flux creep' in these materials.

We will return to the problem of flux jumping in detail in Chap. 6 (Practical Superconductors) and describe how the problem has been solved successfully by providing stability to the conductors carrying several kA current.

3.6.4 Flux Creep

Anderson built up over the critical state model proposed by Bean and modified by Kim and argued that if the critical current J or the field B exceed the critical values in (3.15), flux bundles leak through the material and the material returns to critical state. Flux lines closer than the London penetration depth may be considered bound together via their mutual field interaction and move as flux bundle of dimension $\sim 10^{-5}$–10^{-6} cm. This flux motion has been termed [7] as "flux creep". Anderson gave a theory [7, 8] of flux creep in terms of the thermally activated movement of flux bundle caused by an interplay between the Lorentz force ($J \times B$) and pinning

force. The flux movement is viscous and highly dissipative. Even when the pinning force exceeds the driving force ($FP > FL$), at a finite temperature ($T > 0$ K) the thermal energy associated with the driving force of flux density gradient may force the flux bundles to hop from one pinning centre to another or from one potential well to another potential well. Flux creep is revealed in two ways. One, the trapped magnetic flux shows a slow variation leading to a logarithmic decay [8] of flux with time (t) as

$$\partial B \, \alpha \, k_B T \, \ln(t) \tag{3.16}$$

This creep is unobservably slow unless the flux density gradient is close to the critical value. Second, the flux creep leads to a longitudinal resistive voltages caused by the drifting of the flux bundles under the influence of current flow through the conductor. This voltage is proportional to the average creep velocity of the flux bundle.

The theory of Anderson clearly establishes a marked variation of J_c with temperature in the range of 0.5–0.1 T_c. The movement of flux bundles is blocked at the pinning centres by an energy barrier (potential well). When a field is applied, the flux density in the material is not uniform because of this pinning. In the presence of a transport current the Lorentz force exerts a force on the flux bundles and modify the local free energy which turns the barrier structure spatially 'down hill' direction in a 'stair case' style. The flux bundle jumps over the barrier under thermal excitation at finite temperature below T_c. The bundle jumps at the rate

$$v = v_0 \exp\left[-U(B, T, J)/k_B T\right] \tag{3.17}$$

where v_0 is a characteristic frequency of flux bundle vibration assumed to be 10^5–10^{11} s^{-1} and $U(B, T, J)$ is the activation free energy.

In high T_c oxide superconductors (HTS), to be introduced in the next chapter, the problem of thermally activated flux creep has been found [9–12] to be severe. Several models based upon the classical theory have been developed. Two models, namely, the 'giant flux creep model' [9] and the 'thermally assisted flux flow model' [13] assume the all HTS materials have intrinsically low pinning barriers ($U_0/k_B T_c$) < 10. Here U_0 is the effective pinning potential height and $k_B T_c$ is the thermal energy. The studies have shown that the relaxation is considerably faster in HTS in comparison to the conventional superconductors, though the logarithmic law is followed in both the types of materials. In HTS single crystals, the value of U_0 has been found [9] to be 0.02 eV which is about two orders of magnitude smaller than in conventional metallic superconductors. On the other hand the expected temperature of 77 K for the operation of HTS is high. This makes the height of the pinning barrier ($U_0/k_B T_c$) extremely small which results in 'giant flux creep'. The value of U_0 in practical HTS conductors has been increased significantly by introducing suitable effective pinning centres.

3.6.5 Critical Current by Magnetization

It is possible to calculate critical current density, J_c through the magnetization method using Bean Model [3, 4]. Following expression can be used to calculate J_c from the measured magnetization in increasing and decreasing magnetic field (Fig. 3.13);

$$J_c = 2(M_+ - M_-)/d = 1.59 \times 10^6 \mu_0 \Delta M/d \tag{3.16}$$

where J_c is in A/m^2, $\mu_0 \Delta M = \mu_0(M_+ - M_-)$ is in tesla and d is the diameter of the sample grain in meters. The equation in cgs units reduces to;

$$J_c = 30\Delta M/d \left(\mathrm{A/cm^2}\right) \tag{3.17}$$

where d is in cm.

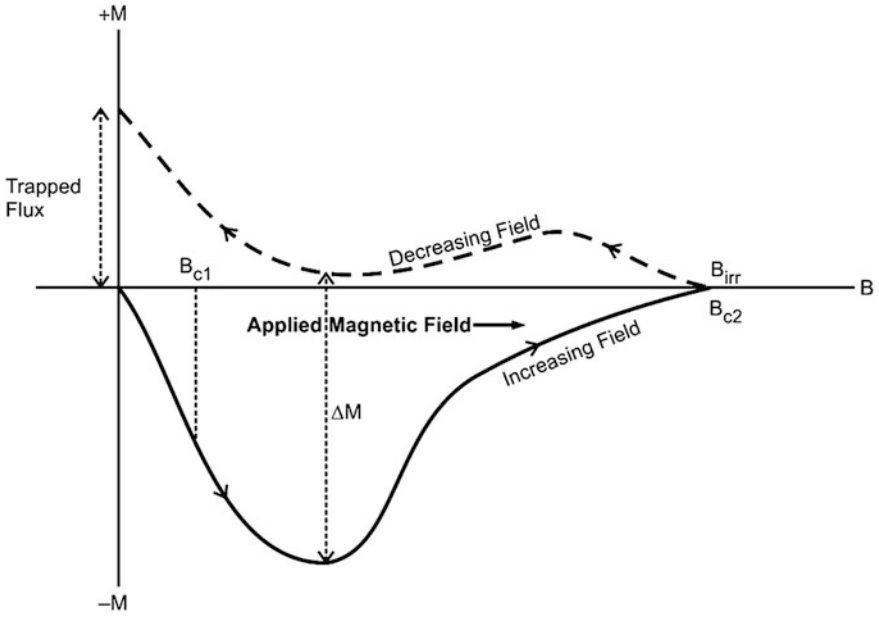

Fig. 3.13 A typical *M–B* plot of a inhomogeneous type II superconductor. J_c can be calculated from the measured ΔM value using the expression (3.17)

3.7 Surface Superconductivity—Critical Magnetic Field B_{c3}

St James and de Gennes [14] in 1963 deduced theoretically that in a finite size superconducting specimen superconductivity exists close to the surface of the superconductor in contact with a dielectric, including vacuum in field higher than B_{c2}. This new critical field is termed as B_{c3} which is 1.695 times B_{c2}. The bulk material though is normal. This superconducting surface layer is found to occur in superconductors with $\kappa > 0.42$ and usually in type II superconductors. B_{c3} depends upon the angle the applied field makes with the surface. It has a maximum value if the field happens to be parallel to the surface and is given by

$$B_{c3} = 2.4\kappa B_c = 1.7\ B_{c2} \tag{3.18}$$

B_{c3} decreases with the angle and is minimum when the applied field is perpendicular to the surface. B_{c3}(min) reduces to B_{c2} for type II superconductors. An indicative magnetic phase diagram (B-κ plots) incorporating B_c, B_{c1}, B_{c2} and B_{c3} has been shown in Fig. 3.14. A type II superconductor now has superconducting state, mixed state, surface superconductivity and the normal state at different field values. Since surface superconductivity occurs for materials with $\kappa > 0.41$ the

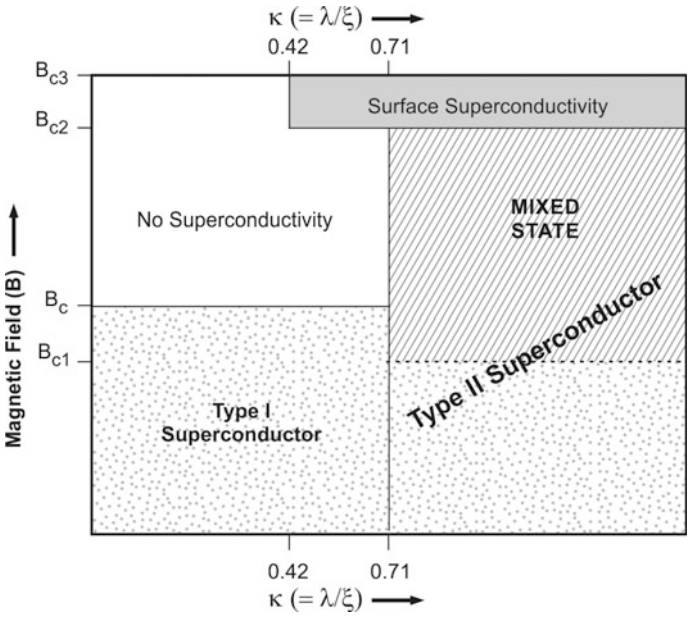

Fig. 3.14 An indicative magnetic phase diagram of a superconductor in contact with a dielectric, showing B-κ plots for B_c, B_{c1}, B_{c2}, and B_{c3} and the existence of surface superconductivity for $\kappa > 0.42$

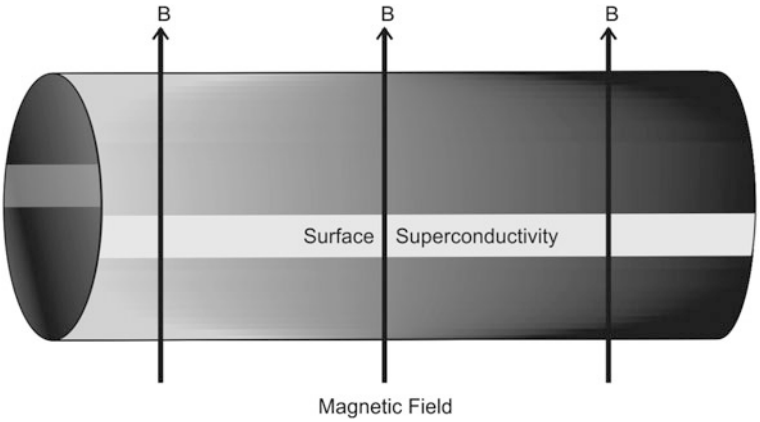

Fig. 3.15 For perpendicular field greater than B_{c2} surface superconductivity reduces to *two strips* parallel to the two sides of the specimen

phenomenon is observed even in Type I superconductors. For example, in Pb, κ increases from 0.37 (at T_c = 7.3 K) to a value of 0.58 at $T < 1.4$ K and surface superconductivity is indeed observed. Surface superconductivity is observed at the interface of the material and a dielectric (or vacuum). Surface superconductivity does not occur at the interface of the superconductor and a metal. So, no surface superconductivity is observed if a type II superconductor is coated with metal. For field higher than B_{c2} the surface layer shrinks to two strips along the length of the specimen. Close to B_{c3} these strips reduce to just two lines where the field happens to be parallel to the surface (Fig. 3.15).

3.8 Paramagnetic Limit

B_{c2} in type II though is high and still increases at reduced temperatures but cannot be increased indefinitely, even if κ too is made high. In fact, the B_{c2} of the best known superconductor is limited to a value much smaller than the predicted one. In high magnetic field the electron spins tend to align themselves along the direction of the field. This lowers the magnetic energy considerably which is not conducive to superconductivity which envisages anti parallel spins to form Cooper pairs. At high enough field it may be energetically favourable for the material to go to normal paramagnetic state rather than remaining in a superconducting state. Experimentally the highest value of B_{c2} has been found limited to what is known as the paramagnetically limited field, $B_p = 1.6 \times 10^6\ T_c$ (A m^{-1}) beyond which superconductivity does not exist, irrespective of how large is the value of κ.

References

1. A.A. Abrikosov, Zh. Eksperim. i. Fiz. **32**, 1442 (1957); Sov. Phys.—JETP. **5**, 1174 (1957)
2. A.C. Rose-Innes, E.H. Rhoderidz, *Introduction to Superconductivity*. Copyright © 1969, Pergamon Press, Library of Congress Catalog Card No. 79-78591
3. C.P. Bean, Phys. Rev. Lett. **8**, 250 (1962)
4. C.P. Bean, Rev. Mod. Phys. **36**, 31 (1964)
5. K. Mendelssohn, Proc. Roy. Soc. (London) **A152**, 34 (1935)
6. Y.B. Kim, C.F. Hemstead, A.R. Strnad, phys. Rev. **129**, 528 (1963)
7. P.W. Anderson, Phys. Rev. Lett. **9**, 309 (1962)
8. P.W. Anderson, Y.B. Kim, Rev. Modern Phys. **36**, 39 (1964)
9. Y. Yashurun, A.P. Malozemoff, Phys. Rev. Lett. **60**, 2202 (1988)
10. T.T.M. Palstra, B. Batlogg, L.F. Schneermeyer, J.V. Waszczak, Phys. Rev. Lett. **61**, 1662 (1988)
11. D. Shi, M, XuA. Umezawa and R.F. Fox. Phys. Rev. **B42**, 2026 (1990)
12. Y. Yashrun, A.P. Malozemoff, T.K. Warthington et al., Cryogenics **29**, 258 (1989)
13. P.S. Kes, J. Aarts, J. van der Berg et al., Supercond. Sci. Technol. **1**, 242 (1989)
14. D. Saint, James and P.G. de Gennes. Phys. Lett. **7**, 306 (1963)